Arch Toxicol (2014) 88:881–892
DOI 10.1007/s00204-014-1194-x

INORGANIC COMPOUNDS

Nickel-induced cell death and survival pathways in cultured renal proximal tubule cells: roles of reactive oxygen species, ceramide and ABCB1

Faouzi Dahdouh · Maximilian Raane · Frank Thévenod · Wing-Kee Lee

Received: 20 September 2013 / Accepted: 9 January 2014 / Published online: 22 January 2014

Abstract Nickel and nickel compounds are carcinogens that target the lungs and kidneys causing cell death or cell survival adaptation. The multidrug resistance P-glycoprotein ABCB1 protects cells against toxic metabolites and xenobiotics and is upregulated in many cancer cell types. Here, we investigated the role of ABCB1 in nickel-induced stress signaling mediated by reactive oxygen species (ROS) and ceramides. In renal proximal tubule cells, nickel chloride (0.1–0.25 mM) increased both ROS formation, detected by 5-(and-6)-carboxy-2′,7′-dichlorodihydrofluorescein diacetate, and cellular ceramides, which were determined by lipid dot blot and surface immunostaining, culminating in decreased cell viability, increased DNA fragmentation, augmented PARP-1 cleavage, and increased ABCB1 mRNA and protein. Inhibitors of the de novo ceramide synthesis pathway (fumonisin B_1, L-cycloserine) and an antioxidant (α-tocopherol) attenuated nickel-induced toxicity as well as induction of ABCB1. ABCB1 protects against nickel toxicity as PSC833, an ABCB1 blocker, augmented the decrease in cell viability by nickel. Moreover, nickel toxicity was attenuated in renal MDCK cells stably overexpressing ABCB1. In agreement with previous data that demonstrated extrusion of (glucosyl)ceramides by ABCB1 (Lee et al. in Toxicol Sci 121:343, 2011), PSC833 increased total cellular ceramides by >2-fold after nickel treatment. Further, glucosylceramide synthase (GCS) mRNA is upregulated by nickel at 3 h by ~1.5-fold but declined with prolonged exposures (6–24 h). Inhibition of GCS with C_9DGJ or knockdown of GCS with siRNA significantly attenuated nickel toxicity. In conclusion, nickel induces a ROS-ceramide pathway to cause apoptotic cell death as well as activate adaptive survival responses, including upregulation of ABCB1, which improves cell survival by extruding proapoptotic (glucosyl)ceramides.

Keywords Sphingolipid · Carcinogenesis · Kidney · ROS

F. Dahdouh · M. Raane · F. Thévenod · W.-K. Lee (✉)
Institute for Physiology, Pathophysiology and Toxicology, Centre for Biomedical Research and Training (ZBAF), Faculty of Health, University of Witten/Herdecke, Stockumer Str. 12, 58453 Witten, Germany
e-mail: wing-kee.lee@uni-wh.de

F. Dahdouh
Department of Biochemistry, Faculty of Sciences, University of Annaba, El-Hadjar, Annaba, Algeria

Introduction

Nickel is omnipresent at low levels in the environment due to its abundance in the earth's crust. Nickel is used in industry for alloys, coins, batteries and electroplating but human industrial activities contaminate the environment resulting in unnatural high levels of nickel. Nickel compounds have been classified as class I carcinogens by the International Agency for Research on Cancer (IARC) (IARC 2012) and induce tumor formation at virtually every site of application in experimental animals. In humans, occupational exposure to acute high levels of nickel primarily leads to diseases of the lung with a high incidence of nasal and lung cancer (Kasprzak et al. 2003). The general nonsmoking population is exposed to nickel compounds via ingestion of contaminated water and foodstuffs and excretion primarily through the urine making the kidney a nickel-exposed organ. In fact, the kidney is a target organ for nickel carcinogenesis (Severa et al. 1995; Sunderman et al. 1979), where nickel is better retained (Smith and Hackley 1968), and an increased risk of kidney cancer occurrence has been associated with nickel exposure (Arena et al. 1998).

Ceramides are sphingolipids that are comprised of a sphingosine backbone and a fatty acid and exist as dynamic pools in the cell. Ceramides were initially thought to be only important in membrane structure but has been indisputably shown to function as a signaling molecule in multiple cellular processes, such as apoptotic cell death, cell survival and cell differentiation. Cellular levels of ceramides are modulated by specialized enzymes (Hannun and Obeid 2008). Metabolism of sphingomyelin, sphingosine or glucosylceramide (GluCer) by sphingomyelinases, ceramide synthases or cerebrosidases, respectively, or activation of the de novo synthesis pathway increases total cellular ceramides. Conversely, ceramide levels can be attenuated through increased activities of ceramidases, ceramide kinases and glucosylceramide synthase (GCS), which convert ceramide to sphingosine, ceramide-1-phosphate and glucosylceramide, respectively. Length of the *N*-acylated fatty acid in ceramides, which defines the different ceramide species, seems to often govern distinct and opposing functions, though this is also context dependent (Hartmann et al. 2012; Mesicek et al. 2010). In a novel observation, cadmium, another carcinogenic heavy metal, was reported by our laboratory to increase total cellular ceramides possibly by de novo synthesis (Lee et al. 2007). This ceramide increase led to augmented intracellular calcium concentrations and in turn activated the calcium-dependent proteases, calpains and culminated in apoptotic cell death. So far, the role of ceramides in Ni^{2+}-induced toxicity or carcinogenesis has not been investigated.

The multidrug resistance P-glycoprotein ABCB1 is responsible for the extrusion of unwanted metabolites and xenobiotics from cells in the liver and kidney leading to excretion from the body via the bile and urine. The expression of ABCB1 is regulated at the transcriptional level, and a multitude of transcription factors has been identified as positive regulators of ABCB1, such as nuclear factor kappa B, TCF4, AP-1 and the more recently identified PITX2 (Scotto 2003; Lee et al. 2013). Aberrant regulation of ABCB1 occurs frequently in tumor cells leading to increased ABCB1 expression, which results in multidrug resistance, attenuated chemotherapeutic efficacy and evasion of apoptosis (Gottesman and Ling 2006; Hanahan and Weinberg 2011). In our previous work, we have demonstrated that ABCB1 was upregulated by cadmium in correlation with improved cell survival that was a consequence of increased extrusion of ceramides by ABCB1 (Lee et al. 2011; Thévenod et al. 2000). These observations prompted us to ask whether this mechanism for apoptosis evasion and improved cell survival is applicable to other carcinogenic heavy metals.

In this study, we find that Ni^{2+} activates the same mechanisms, that is, ceramide formation and extrusion of ceramides by upregulated ABCB1 to prevent cell death of kidney proximal tubule cells (PTCs). Furthermore, we show that induction of cell death by Ni^{2+} is not limited to ceramides but GluCer is also involved.

Materials and methods

Cell culture, treatments and siRNA transfection

The immortalized p53-deficient rat kidney proximal tubule cell line derived from the S1 segment (WKPT-0293 Cl.2) was cultured as reported elsewhere (Lee et al. 2011; Bork et al. 2010) and used at passages <50. Unless otherwise indicated, cells were grown for 2 days prior to treatment with inhibitors and/or 0.1–0.25 mM $NiCl_2$ in serum-free medium. $NiCl_2$ (Sigma-Aldrich, purity 98 %) was dissolved in water to a concentration of 100 mM. Inhibitors used were (concentration and preincubation time): PSC833 (0.1–1 μM, 15 min) (a gift from Sanofi-Aventis), L-cycloserine (100 μM, 2 h) (Alexis Biochemicals), fumonisin B_1 (3 μM, 2 h) (Alexis Biochemicals), C_9DGJ (2 μM, 48 h) (Toronto Research Chemicals Inc.) and α-tocopherol (100 μM, 1 h) (Sigma-Aldrich).

Madin-Darby canine kidney (MDCK) cells stably overexpressing human MDR1/ABCB1 were obtained from Dr. Michael M. Gottesman and cultured as previously described (Lee et al. 2011).

Glucosylceramide synthase (GCS) siRNA was purchased from Dharmacon (Thermo Fisher Scientific) and transfected into cells using Lipofectamine RNAiMAX (Invitrogen) according to manufacturer's instructions. WKPT-0293 Cl.2 cells (2×10^4) were transfected with 25 nM control siRNA (Eurogentec) or GCS siRNA 1 day after plating. Medium was changed after 24 h, and cells were used for further analyses after 66 h for MTT assay and 72 h for mRNA analysis.

Cell death assays

Cell viability was determined by MTT, which was performed as described elsewhere (Thévenod et al. 2007; Chakraborty et al. 2010). Cellular DNA fragmentation was used as an indication of apoptosis and measured using a cellular DNA fragmentation ELISA (Roche) following manufacturer's instructions.

Reverse transcriptase PCR

Isolation of total RNA, synthesis of cDNA and PCR reactions were performed. Primers and cycling protocols are listed in Table 1. Gel documentation and densitometry analysis were performed using Image Lab Software 3.0 (Bio-Rad Laboratories) with correction for loading using housekeeping genes.

Table 1 PCR primers and cycling protocols

Primer	Sequence (5′–3′)	Annealing temperature (°C)	No. of cycles	Product size (bp)
Rat GCS forward	TTGTTCGGCTTCGTGCTCTT	55	25	410
Rat GCS reverse	GACTCGTATTCCGCTATCAC			
Rat Abcb1a forward	GATGGAATTGATAATGTGGACA	56	33	351
Rat Abcb1a reverse	AAGGATCAGGAACAATAAA			
Rat Abcb1b forward	GGACAGAAACAGAGGATCGC	55	35	356
Rat Abcb1b reverse	TCAGAGGCACCAGTGTCACT			
Rat Gapdh forward	AATGCATCCTGCACCACCAACTGC	61.9	18	300
Rat Gapdh reverse	GCGGCATGTCAGATCCACAACGG			

Immunoblotting

SDS-PAGE and immunoblotting of ABCB1 using C219 antibody (1:200, Alexis Biochemicals), PARP1 (1:2,000, Cell Signaling Technology) and β-actin (1:5,000, Sigma-Aldrich) have been described elsewhere (Lee et al. 2011; Lee et al. 2012).

Surface immunofluorescence staining

Live surface staining of unfixed cells was executed as previously described (Lee et al. 2013). Mouse anticeramide IgM antibody (clone 15B4, Alexis Biochemicals) was used at 1:100. Secondary A488-coupled antimouse IgM antibody (Jackson Laboratories) was used at 1:600.

Detection of reactive oxygen species

The nonfluorescent general oxidative stress detector 5-(and-6)-carboxy-2′,7′-dichlorodihydrofluorescein diacetate (carboxy-H_2DCFDA) fluoresces when oxidized by H_2O_2, peroxyl radicals and peroxynitrite anion (Invitrogen). Experiments were performed as previously described (Chakraborty et al. 2010).

Ceramide dot blot

Total lipids were extracted from equal amounts of cells using the method of Bligh and Dyer (1959; Perry et al. 2000). Following protein determination by the method of Bradford (1976), 100 µg protein was diluted to 400 µl with buffered saline solution (BSS), added to 1.5 ml $CHCl_3$:CH_3OH (1:2, v/v) and vortexed for 15 s. $CHCl_3$ (0.5 ml) and BSS (0.5 ml) were added in succession with 15 s vortexing after each step. Phases were given 10 min to separate, and tubes were centrifuged at 4,444*g* for 5 min at 20 °C. The upper aqueous phase was carefully removed, and the organic phase was transferred to new glass tubes, which had been cleaned with $CHCl_3$. Lipids were dried under a constant stream of nitrogen and reconstituted in $CHCl_3$. Lipids (1 µl) were dotted onto Whatman nitrocellulose membranes, air-dried and blocked for 1 h in 0.2 M NaCl, 50 mM Tris–HCl, pH 7.4 containing 10 % nonfat milk at room temperature. Primary mouse anticeramide IgM (clone S58-9) antibody (Glycobiotech GmbH, Kükels, Germany) was used at 1:5,000 in 3 % nonfat milk and incubated overnight at 4 °C. Horseradish peroxidase-conjugated antimouse IgM (Santa Cruz) was diluted 1:2,500 and incubated for 1 h at 4 °C. Dot blots were developed using Western Lightning enhanced chemiluminescence (Perkin Elmer) and blue X-ray films (Kodak). Densitometry analysis was performed using TINA v2.09 software (Raytest GmbH, Straubenhardt, Germany).

Statistical analyses

Unless otherwise indicated, experiments were performed a minimum of three times and are displayed as mean ± SE of the mean. Pairwise comparisons were tested for statistical significance by unpaired Student's *t* test. Comparisons of multiple groups were tested by one-way ANOVA with Tukey post hoc test. Statistical tests were performed using SigmaPlot or GraphPad Prism where $p < 0.05$ was considered significant.

Results

Nickel signals stress response and cell death through oxidative stress and ceramides

Activation of cell stress leads to activation of adaptive responses that determine cell fate. To investigate the potency of nickel chloride in renal PTCs, a dose response curve was generated after 6 and 24 h incubation with Ni^{2+}, and cell viability was determined using MTT assay. As shown in Fig. 1a, no significant change in cytotoxicity by Ni^{2+} was observed after 6 h. In contrast, after 24 h, cell viability was decreased by ~40 % at the lowest concentration tested 0.1 mM Ni^{2+}. Cell viability decreased in

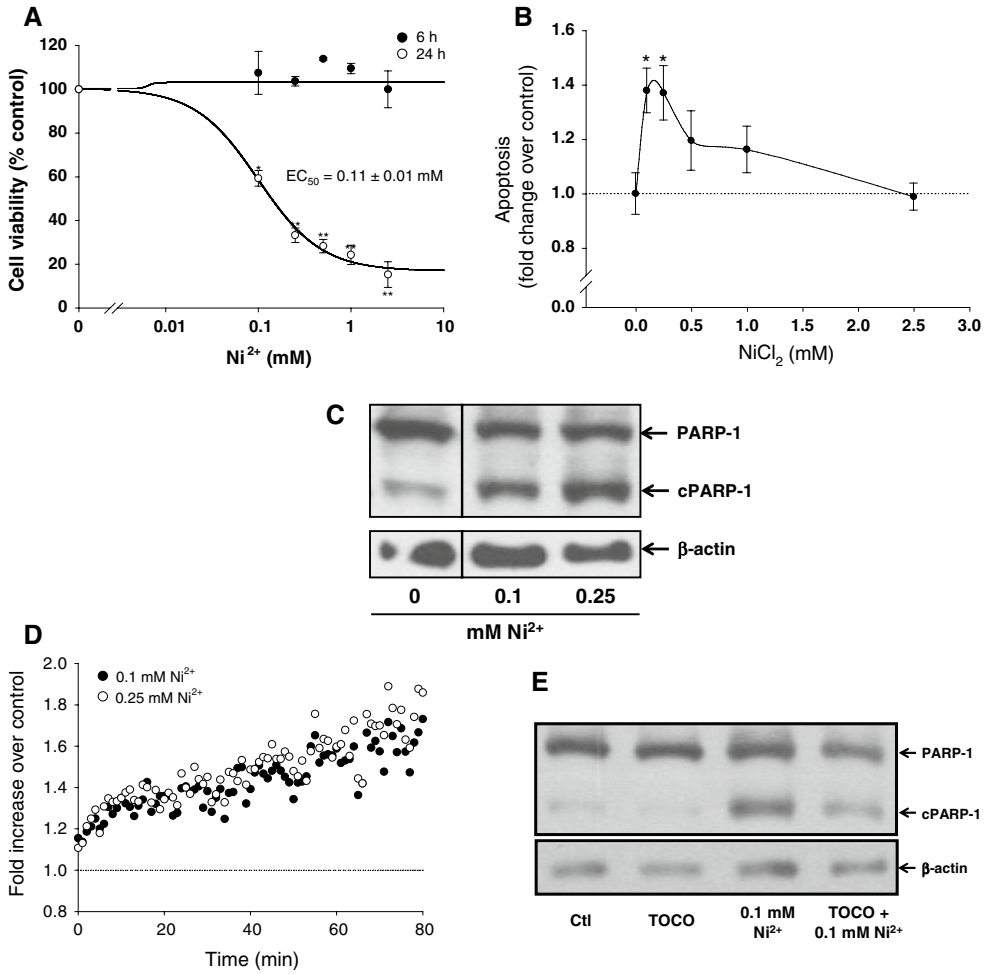

Fig. 1 Nickel decreases cell viability and increases apoptosis by oxidative stress. **a** MTT assay was performed in PTCs exposed to varying concentrations of Ni^{2+} in serum-free medium ($n = 3$–9). Student's unpaired t test compares cell viability at 6–24 h where $*p < 0.05$ and $**p < 0.01$. **b** Apoptosis was assessed by intracellular DNA fragmentation in adherent PTCs following Ni^{2+} treatment in serum-free medium for 24 h ($n = 4$). One-way ANOVA compares Ni^{2+}-treated PTCs to control cells where $*p < 0.05$. **c** Cleavage of PARP-1 (cPARP-1) was determined by immunoblotting. Image is representative of three independent experiments (*different lanes from the same blot are shown*). **d** Increase in ROS levels was monitored using the redox reactive dye carboxy-H_2DCFDA. PTCs loaded with carboxy-H_2DCFDA were brought into suspension and incubated with Ni^{2+}. DCF fluorescence was measured immediately at excitation/emission 500/535 nm for up to 80 min. Graph is a representative of two independent experiments. **e** PARP-1 cleavage in Ni^{2+}-treated PTCs ± 100 μM α-tocopherol (TOCO). Immunoblot is a representative of two independent experiments

a concentration-dependent manner by Ni^{2+} after 24 h with an $EC_{50} = 0.11 \pm 0.01$ mM ($n = 8$). These data indicate that the toxic effects of Ni^{2+} are somewhat delayed, which could be explained by limited entry of Ni^{2+}, the time it takes for accumulation of Ni^{2+} into intracellular compartments in order for its effects to be elicited or activation of antagonizing survival pathways. Since the MTT assay does not discriminate between apoptosis, necrosis and cell proliferation, cellular DNA fragmentation and PARP-1 cleavage were used as indicators of apoptosis. Using an assay to detect intracellular DNA fragmentation in adherent cells, apoptosis was maximally increased by 0.1 and 0.25 mM Ni^{2+} to almost 1.4-fold over nontreated controls (Fig. 1b). The rate of apoptosis diminished with increasing Ni^{2+} concentrations, suggesting that the loss of cell viability at higher Ni^{2+} concentrations recorded in Fig. 1a is due to necrotic cell death or detachment of cells. The apoptosis-inducing effect of Ni^{2+} at 0.1–0.25 mM was confirmed by immunoblotting for PARP-1, which is cleaved by active caspase-3 thus preventing repair of DNA damage. As shown in Fig. 1c, full-length PARP-1 decreases with Ni^{2+} and cleaved PARP-1 increases accordingly. To further investigate the role of Ni^{2+} in renal PTCs, 0.1 and 0.25 mM Ni^{2+} concentrations were used, which reduced cell viability to 59.3 ± 3.6 and 33.3 ± 3.3 % after 24 h, respectively (Fig. 1a).

Oxidative stress and DNA damage are two well-documented cellular changes brought about by Ni^{2+} that contribute to toxicity and carcinogenesis (Kasprzak et al. 1997). Here, we could confirm that Ni^{2+} increases the formation of ROS that may lead to stress, survival and ultimately cell death in renal PTCs. In Fig. 1d, ROS formation by Ni^{2+} was immediate and continued to increase further with time up to ~1.8-fold over controls after 80 min. ROS can act as signal messengers within the cell and have been reported to be important for cell death induction as well as the stress response that contributes to carcinogenesis (Gupta et al. 2012; Yang et al. 2013). Using the membrane permeable antioxidant α-tocopherol, or vitamin E, decrease in cell viability by Ni^{2+} was partly but significantly attenuated (Table 2). The effect of α-tocopherol on preventing Ni^{2+}-induced apoptosis was confirmed by PARP-1 immunoblots. The presence of α-tocopherol reduced the amount of cleaved PARP-1 by 0.1 mM Ni^{2+} (Fig. 1e).

The increased formation of ROS leads to the activation of myriad downstream signaling cascades, including the sphingolipid ceramide pathway, which is intimately connected to ROS. Here, two commercially available ceramide antibodies were used to detect endogenous ceramides. With the antibodies, not only can total cellular ceramides be measured but the distribution of ceramides can be investigated. The specificity of these antibodies for ceramides has been previously scrutinized and has been the subject of intense investigation (Cowart et al. 2002; Vielhaber et al. 2001; Grassme et al. 2001). The S58-9 IgM clone from Glycobiotech was found to be ceramide specific in lipid dot blot and overlay assays with little to no reaction with sphingomyelin, phosphatidylcholine or sphingosine, whereas the 15B4 IgM clone is less specific in these assays (Cowart et al. 2002; Vielhaber et al. 2001). We could corroborate these findings: the 15B4 clone did not detect ceramides in the lipid dot blots, whereas the S58-9 clone did. Further, the S58-9 clone had much higher affinity for natural long-chain brain ceramides than for short-chain C_6-ceramide (data not shown). However, the 15B4 clone proves to be more suitable for detecting ceramides in an in vivo, and not in vitro, environment that is supported by the use of the antibody in detecting surface ceramide on the plasma membrane (Grassme et al. 2001). In light of the differing suitability of each antibody clone, the 15B4 IgM was used for surface immunostaining studies and the S58-9 IgG clone was used exclusively for lipid dot blot assays.

To ascertain whether Ni^{2+} increases ceramide formation, live surface immunostaining of renal PTCs exposed to 0.1 mM Ni^{2+} was performed after 24 h. Without fixation or permeabilization of the cells, the 15B4 antibody detects the presence of ceramide in the outer leaflet of the lipid bilayer (Grassme et al. 2001). As seen in Fig. 2a, virtually no ceramide was present on the cell surface in control cells. In contrast, Ni^{2+} treatment strongly induced an increase in surface ceramide in cells with and without apoptotic nuclei. Quantification of the ceramide fluorescence signal confirmed a significant increase of ceramide by Ni^{2+} with a ~6.7-fold increase over controls (% threshold area 0.35 ± 0.16 % in controls, 2.30 ± 0.64 % in Ni^{2+}-treated) (Fig. 2a). Ceramide dot blots were executed to complement these observations. Total cellular ceramides increased in 0.1 mM Ni^{2+}- and 0.25 mM Ni^{2+}-treated cells by 2.26 ± 0.5-fold and 2.99 ± 0.8-fold, respectively, further confirming the novel finding that ceramides are increased by Ni^{2+} (Fig. 2b).

How is ceramide metabolism affected by Ni^{2+} in order to increase total cellular ceramides? The simplest mechanism is engagement of the de novo ceramide synthesis pathway to increase total ceramide levels. Inhibitors of the de novo synthesis pathway were used, and their effects on Ni^{2+}-induced decrease in cell viability were examined. Fumonisin B_1 is a potent inhibitor of ceramide synthase, which is not only involved in the de novo ceramide synthesis pathway but also in the salvage pathway where ceramide is formed from sphinganine. Fumonisin B_1 significantly improved cell viability to 71.8 ± 7.2 % from 52.3 ± 7.5 % in Ni^{2+} only cells (Table 2) as well as reducing the occurrence of cleaved PARP-1 (Fig. 2c). To confirm that the de novo synthesis pathway is responsible for Ni^{2+}-induced ceramide formation, an inhibitor of serine palmitoyltransferase, an enzyme specific to de novo ceramide generation, L-cycloserine was employed. Likewise, L-cycloserine augmented cell viability from 61.3 ± 6.8 % in Ni^{2+} only cells to 71.4 ± 5.8 % (Table 2), substantiating the involvement of the de novo ceramide synthesis pathway in Ni^{2+}-induced ceramide formation.

Table 2 Nickel-induced cell death is prevented by an antioxidant and inhibitors of the ceramide synthesis pathway

Target	Inhibitor name	Concentration	Cell viability (% control)			
			Inhibitor	0.1 mM Ni^{2+}	Inhibitor + Ni^{2+}	Significance
Lipid peroxidation	α-Tocopherol	100 μM	91.0 ± 2.3	55.3 ± 6.7	77.1 ± 5.4	0.012 ($n = 8$)
Ceramide synthase	Fumonisin B_1	3 μM	89.1 ± 2.7	52.3 ± 7.5	71.8 ± 7.2	0.045 ($n = 6$)
Serine palmitoyltransferase	L-Cycloserine	100 μM	84.3 ± 6.3	61.3 ± 6.8	71.4 ± 5.8	0.0007 ($n = 8$)
Glucosylceramide synthase	C_9DGJ	2 μM	96.5 ± 4.1	58.4 ± 6.4	70.7 ± 4.4	0.042 ($n = 5$)

Cell viability was determined with the MTT assay after 24 h with Ni^{2+} . Statistical significance was tested between Ni^{2+} and inhibitor + Ni^{2+}

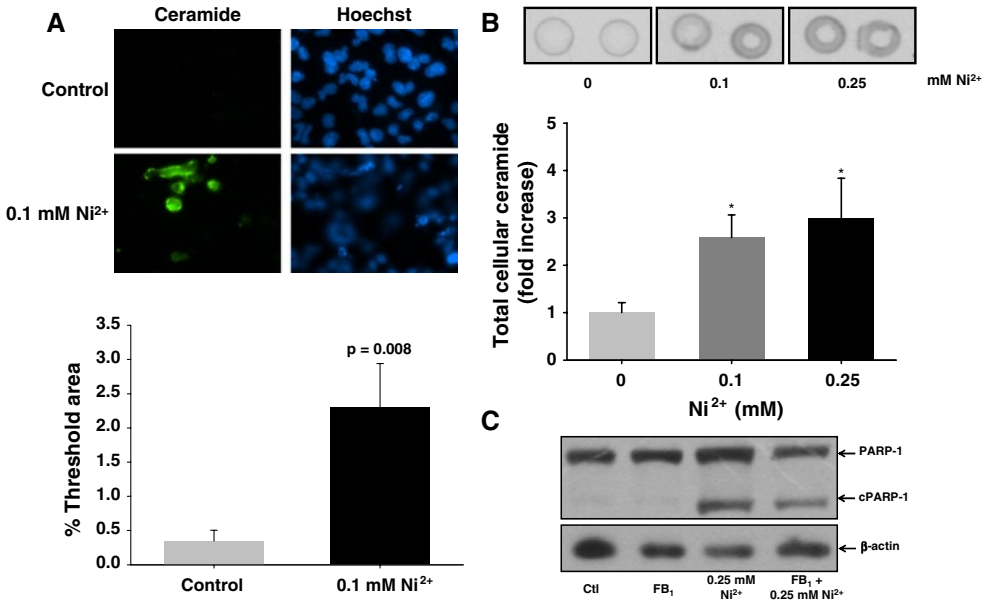

Fig. 2 Nickel increases ceramide formation to induce apoptosis. **a** Live surface immunofluorescence staining for ceramide using the 15B4 anticeramide IgM antibody was performed on PTCs exposed to Ni^{2+} for 24 h. Quantitative analysis of % threshold area demonstrated a significant increase in surface ceramide ($n = 3$). **b** Increase in cellular ceramides by Ni^{2+} after 24 h was confirmed with lipid dot blots using the S58-9 anticeramide IgM antibody. Total lipids were extracted from PTCs, reconstituted in $CHCl_3$ and dot blotted (1 μl) onto nitrocellulose membranes. Densitometry analysis was performed ($n = 3$–6). *$p < 0.05$. **c** PARP-1 cleavage in Ni^{2+}-treated PTCs ± 3 μM fumonisin B_1 (FB_1). Immunoblot is a representative of two independent experiments

Nickel-induced reduction in cell viability is associated with increased ABCB1

ABCB1 is also a well-known cell stress response gene and is upregulated by a variety of toxic metals, including cadmium (Thévenod et al. 2000) and arsenite (Chin et al. 1990). Here, we show that ABCB1 is augmented by Ni^{2+} exposure after 24 h in renal PTCs. At the mRNA level, rodent Abcb1a responds stronger than Abcb1b. Abcb1a increases by 2.6 ± 0.2-fold and 2.2 ± 0.3-fold after exposure to 0.1 and 0.25 mM Ni^{2+}, respectively (Fig. 3A). Furthermore, ABCB1 protein was augmented by Ni^{2+} after 24 h as determined by immunoblotting (Fig. 3b). At the lowest concentration tested of 0.05 mM Ni^{2+}, no significant increase in ABCB1 was observed, whereas 0.1 and 0.25 mM Ni^{2+} increased ABCB1 protein by 2.5 ± 0.7-fold and 4.9 ± 1.3-fold, respectively. Interestingly, with 0.25 mM Ni^{2+}, multiple bands increased in intensity compared to control (Fig. 3b, arrowheads). The ABCB1 protein is heavily glycosylated, which is essential for proper folding and insertion into the plasma membrane (Schinkel et al. 1993). The lower molecular weight band indicates an unglycosylated form of ABCB1 that could be the result of a high rate of ABCB1 protein synthesis, such that there is backflow of immature ABCB1 that is yet to be glycosylated and inserted into the plasma membrane. An alternative explanation is that nickel inhibits the enzymes responsible for glycosylation. Though there is no clear evidence for heavy metals directly affecting glycosylation enzymes, one study showed that nickel played a role in deglycosylation of 2′-deoxyguanosine that required hydrogen peroxide and ascorbate (Littlefield et al. 1991). However, this matter requires further clarification.

Interestingly, α-tocopherol could also partially inhibit the increase in ABCB1 by Ni^{2+} at the protein level by ~50 % (Fig. 3c, d), further strengthening the dual role of ROS in cell death and survival. Similarly, lowering ceramide formation by ceramide synthase inhibition through fumonisin B_1 could attenuate the increase in ABCB1 by Ni^{2+} (Fig. 3c, d). These data imply that both ROS and ceramide are not only involved in signaling cell death but also participate in the adaptive cell stress response.

Inhibition of ABCB1 exacerbates nickel-induced toxicity by increasing cellular ceramides

The increased expression of ABC efflux transporters, such as ABCB1, is a key characteristic in the development of multidrug resistance of cancer cells (Gottesman et al. 2002; Hanahan and Weinberg 2011), propagating cell survival and evasion of apoptosis. In order to identify the protective effect of ABCB1 against Ni^{2+}-induced cell death, renal MDCK cells stably overexpressing ABCB1 were employed. Using the MTT assay, decrease in cell viability by Ni^{2+} was determined. Figure 4a shows that 0.25 mM

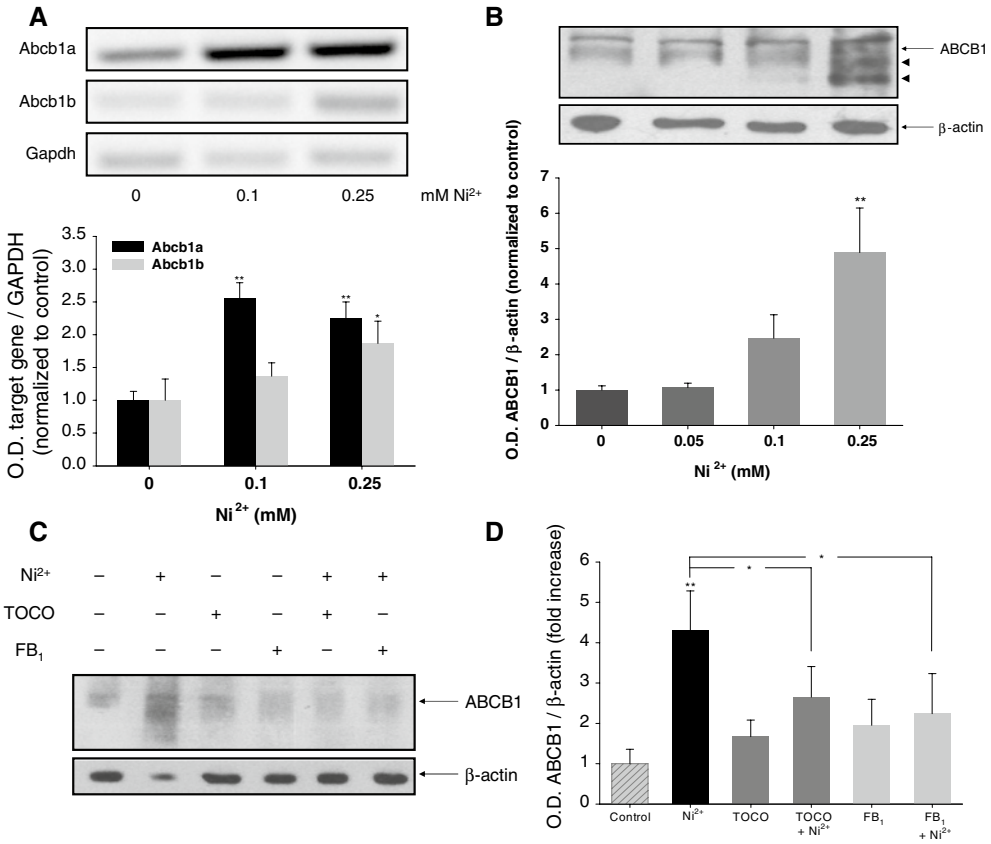

Fig. 3 Nickel-induced upregulation of ABCB1 expression is signaled through ROS, and de novo ceramide synthesis. ABCB1 expression was increased after 24 h treatment with Ni^{2+} as shown by semi-quantitative PCR for Abcb1a and Abcb1b mRNA ($n = 6$) (**a**) and immunoblotting for ABCB1 protein ($n = 3$) (**b**). Densitometry analysis was performed using TINA v2.0. (**c**, **d**) Inhibitors of oxidative stress α-tocopherol (TOCO; 100 μM) and ceramide synthesis fumonisin B_1 (FB_1; 3 μM) were preincubated prior to addition of 0.25 mM Ni^{2+} for 24 h in PTCs. ABCB1 expression was determined by immunoblotting using C219 antibody, and densitometry analysis was performed ($n = 8$). $*p < 0.05$, $**p < 0.01$

Ni^{2+} caused only 5.7 ± 5.2 % reduction in cell viability of ABCB1-MDCK cells but 28.2 ± 3.5 % in parental MDCK cells, which was statistically significant. The same tendency was observed with 0.1 mM Ni^{2+}, but the difference between MDCK and ABCB1-MDCK cells was not significant. Recent work from our laboratory evidenced a transport role of ABCB1 for (glucosyl)ceramides (Lee et al. 2011). To show whether ABCB1 induced by Ni^{2+} also served the same purpose in preventing cell death by extrusion of pro-apoptotic ceramides, the ABCB1 inhibitor PSC833 was utilized. Preincubation of renal PTCs with 1 μM PSC833 prior to 0.1 mM Ni^{2+} treatment for 24 h significantly decreased cell viability further (50.0 ± 1.2 %) than Ni^{2+} treatment alone (59.4 ± 1.7 %). A similar decrease was observed for 0.25 mM Ni^{2+} (Fig. 4b).

To further investigate whether ceramides are extruded by ABCB1 upregulated by Ni^{2+}, total cellular ceramides in the presence of PSC833 were determined by lipid dot blot. Renal PTCs were preincubated with 1 μM PSC833 followed by Ni^{2+} treatment for 24 h. In Fig. 4c, 0.1 mM Ni^{2+} increases cellular ceramides by 2.0 ± 0.3-fold, which is significantly increased to 4.1 ± 0.6-fold in the presence of PSC833. Similarly, PSC833 increased cellular ceramides by 0.25 mM Ni from 3.1 ± 0.7-fold to 5.9 ± 0.9-fold. Previous reports have hypothesized that PSC833 itself can increase ceramides in MCF7 breast cancer cells (Cabot et al. 1998). In contrast, we did not observe a significant increase in PSC833 alone compared to nontreated renal PTCs (0.7 ± 0.2-fold). This discrepancy could lie in the cancer cell phenotype of MCF7 cells. In conclusion, Ni^{2+}-treated renal PTCs augment ABCB1 expression in an attempt to protect themselves against proapoptotic ceramides through ABCB1-mediated ceramide extrusion.

Glucosylceramide has cell death-inducing properties

Ceramide and sphingosine have been extensively shown to be cell death-inducing sphingolipid moieties, whereas

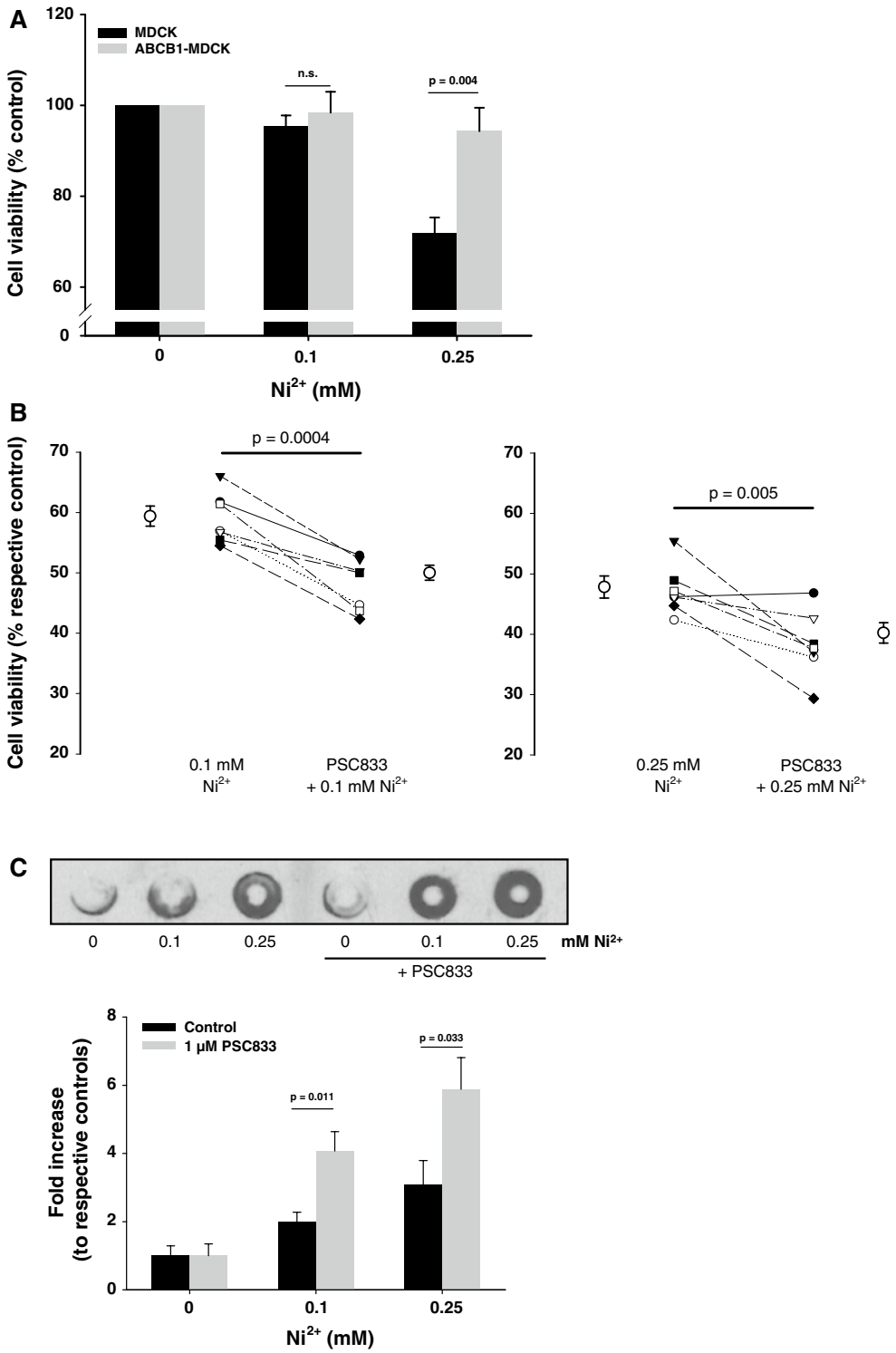

Fig. 4 ABCB1 protects against nickel-induced cell death. **a** ABCB1 overexpressing MDCK cells and their parental MDCK cell line were incubated with Ni^{2+} for 24 h, and cell viability was determined by MTT assay ($n = 3$–7). **b** PTCs were preincubated with 1 μM PSC833 for 15 min followed by Ni^{2+} for 24 h. Cell viability was measured by MTT assay and compared to respective controls. For each Ni^{2+} concentration, seven independent experiments are plotted ±1 μM PSC833 and flanked by the respective mean ± SE. Cell viability in PSC833 alone treated cells was 86.0 ± 2.1 %. **c** PTCs were preincubated with 1 μM PSC833 and then exposed to Ni^{2+} for 24 h. Total lipids were extracted, and cellular ceramides were analyzed by lipid dot blot. Densitometry analysis was performed using TINA v2.0 ($n = 5$). PSC833 alone cells contained 0.71 ± 0.17-fold cellular ceramides compared to controls

sphingosine-1-phosphate is considered antiapoptotic. The role of GluCer in cell death is unclear. To ascertain a role for GluCer in Ni^{2+}-induced cell death, we first assessed the mRNA levels of the GluCer-synthesizing enzyme GCS in response to Ni^{2+} (Fig. 5a). GCS was increased by 0.1 mM Ni^{2+} at early time points of 1–3 h, which reached significance at 3 h (1.46 ± 0.13-fold, $n = 4$). Interestingly, GCS mRNA significantly decreased with prolonged exposures of 6 h and 24 h (0.78 ± 0.08-fold and 0.62 ± 0.04-fold, respectively, $n = 4$).

An increased ceramide pool should drive the formation of downstream ceramide metabolites, such as GluCer or sphingosine and sphingosine-1-phosphate. The degradation pathway appears to be activated by 0.1 mM Ni^{2+} after 24 h since both sphingosine and sphingosine-1-phosphate were increased by up to twofold in mass spectrometry analysis (Lee, W.K. and Thévenod, F., unpublished observations). Since glycosphingolipids are substrates of ABCB1 (Lee et al. 2011; Eckford and Sharom 2005), we hypothesized that GluCer could have a role in cell death. Using pharmacological means, preincubation of renal PTCs with 2 μM C_9DGJ, a GCS blocker, protects against decrease in cell viability by 0.1 mM Ni^{2+} (Table 2), indicating that GluCer has a cell death-inducing ability. This was further supported by a reduction in Ni^{2+}-induced cell death when GCS was knocked down using specific siRNA. A control PCR demonstrates that GCS is effectively knocked down (Fig. 5b). After 66 h of siRNA incubation, renal PTCs were exposed to Ni^{2+} for 24 h and cell viability was determined by MTT assay. With 0.1 mM Ni^{2+}, control siRNA cells exhibited 66.4 ± 4.5 % cell viability, whereas in GCS siRNA cells, 78.2 ± 5.1 % cell viability was observed ($n = 6$). However, this did not reach statistical significance. A similar improvement in cell viability in GCS siRNA cells was measured with 0.25 mM Ni^{2+}. Control siRNA cells displayed 46.5 ± 5.7 % viability after 24 h exposure to 0.25 mM Ni^{2+}, which was significantly improved in GCS siRNA cells to 66.1 ± 6.2 % viability ($n = 6$) (Fig. 5c). Taken together, these data indicate that both ceramide and glucosylceramide are toxic sphingolipid moieties that can induce apoptosis.

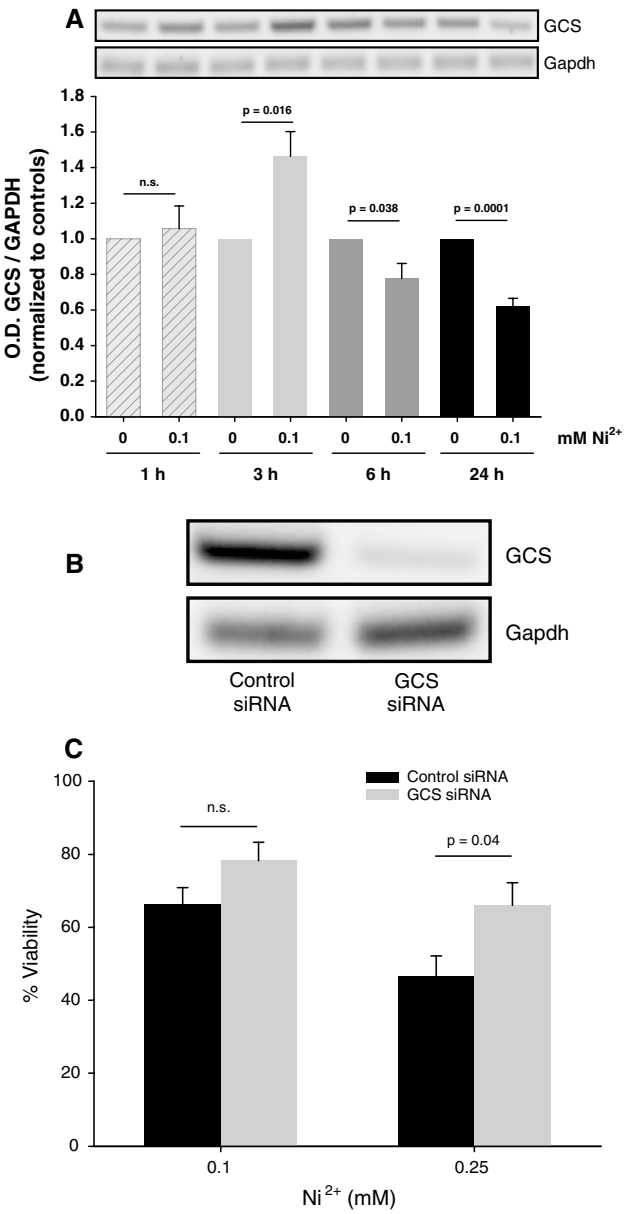

Fig. 5 Glucosylceramide contributes to nickel-induced cell death. **a** Glucosylceramide synthase (GCS) mRNA was determined in response to 0.1 mM Ni^{2+} over a time course of 1–24 h in PTCs by semi-quantitative RT-PCR and densitometry analysis ($n = 4$). **b** GCS mRNA was reduced by a pool of four siRNA sequences directed against rat GCS mRNA that was confirmed by PCR after 72 h. **c** MTT assay demonstrates that knockdown of GCS partially rescues renal cells from Ni^{2+} toxicity after 24 h. Cell viability is plotted as a percentage of nontreated controls ($n = 6$–8)

Discussion

In the present study, we have demonstrated a novel mechanism for nickel toxicity and survival. Alike other carcinogenic metals, Ni^{2+} activates cell stress pathways that bring about adaptive changes in the cell's molecular makeup leading to enhanced cellular survival. Here, nickel evoked an increase in stress signals, in the form of ROS and total cellular ceramides, which were at the nexus of downstream death and survival pathways. Further, proapoptotic ceramides were extruded by the multidrug resistance P-glycoprotein ABCB1 to promote cell survival and potential tumorigenesis.

To enter cells, nickel soluble salts have to compete with the magnesium transport system for uptake and cause cytotoxicity (Costa 2000). It has also been suggested that nickel

is able to exert its toxic effects from outside the cell by inducing an increase in cytosolic calcium (Salnikow et al. 1999b). Cortijo and colleagues convincingly evidenced that the calcium sensing receptor (CaSR) (Cortijo et al. 2010) was involved in transmitting the nickel signal, probably through direct nickel binding (Handlogten et al. 2000), using pharmacological inhibitors and siRNA against the CaSR. Further, using the inhibitor 2-aminoethoxydiphenyl borate to block the inositol triphosphate receptor, the increase in intracellular calcium by nickel was abolished.

Both calcium and ROS formation are intimately involved with ceramide formation in apoptosis induction (Lee et al. 2007; Won and Singh 2006; Park et al. 2010). Here, we are the first to report that nickel can modulate sphingolipid pools. Total cellular ceramides as well as surface ceramides were increased by nickel (Fig. 1). ROS formation was associated with increased ceramides leading to nickel-induced apoptotic cell death, which was attenuated by α-tocopherol and FB_1/L-cycloserine, respectively (Figs. 1, 2, Table 2). Interestingly, the inhibitors employed could only restore cell viability to maximally ~70 % (Table 2, "Inhibitor + Ni^{2+}" column), which implies that ROS and ceramide could be part of the same signaling cascade. ROS has been previously reported to be involved in inducing apoptosis by nickel in kidney proximal tubule cells. An increase in ROS formation precedes DNA damage, increase in proapoptotic Bax and Bad, mitochondrial dysfunction and activation of the intrinsic apoptotic pathway (Wang et al. 2012; Kasprzak et al. 1997; Lee et al. 2001). It remains to be investigated whether intracellular calcium is involved in nickel-induced cell death of kidney cells.

ABCB1 was increased by nickel exposure at the transcriptional level (Fig 3a). A number of transcription factors known to regulate ABCB1 (Scotto 2003) have been shown to respond to nickel, including nuclear factor kappa B (Ding et al. 2009; Cruz et al. 2004), activator protein 1 (AP-1) (Cruz et al. 2004; Ding et al. 2009), p53 (Salnikow et al. 1999a) and hypoxia-inducible factor 1 (HIF-1) (Salnikow et al. 1999a). Furthermore, some of these transcription factors are activated by upstream ROS formation resulting in ABCB1 upregulation, for example nuclear factor kappa B (Thévenod et al. 2000), which could be applicable for nickel. Of note, not all ROS-transcription factor connections positively regulate ABCB1 (Wartenberg et al. 2003). We have previously shown that cadmium activates the β-catenin/T-cell factor 4 (TCF4) pathway to increase ABCB1 expression by disrupting E-cadherin adherens junctions and releasing β-catenin, which then translocates to the nucleus (Chakraborty et al. 2010; Thévenod et al. 2007). In contrast, nickel does not appear to use this pathway since β-catenin distribution, TCF4 mRNA and TCF4 transcriptional activity were unchanged by 0.1–0.25 mM Ni^{2+} compared to controls after 24 h (data not shown). The specificity of β-catenin/TCF4 pathway to cadmium may lie in its ionic radius similarity to Ca^{2+} (Cd^{2+}, 0.097 nm versus Ca^{2+}, 0.099 nm), which maintains the adherens junctions structure, leading to displacement of Ca^{2+}, redistribution of β-catenin to the nucleus and activation of TCF4 transcription (Chakraborty et al. 2010; Thévenod et al. 2007). The ionic radius of nickel (0.069 nm) does not permit this action of molecular mimicry.

In addition to transcriptional regulation, there is extensive evidence that nickel modulates gene expression at the epigenetic level by altering the DNA methylation status (Brocato and Costa 2013). DNA methylation may affect transcription either by hindering the accessibility of transcription factors or by forming compact inactive chromatin, named heterochromatin, through modulation of histones by recruitment of proteins, such as histone deacetylases. In cancer cells, the pattern of DNA methylation is reversed compared to normal tissue (Baylin 2005). Nickel has been shown to induce de novo DNA methylation, and $NiCl_2$ or $Ni(CH_3COO)_2$ regulates gene expression through histone deacetylation (gene repression) (Golebiowski and Kasprzak 2005) or histone dimethylation (H3K9) (Chen et al. 2006) and histone trimethylation (H3K4) (gene activation) (Tchou-Wong et al. 2011). ABCB1 can be regulated by epigenetic changes, namely increased H3K4 acetylation (Toth et al. 2012) and H3K4 methylation (Baker et al. 2005) both resulting in augmented ABCB1 expression and MDR phenotype. Nickel has a yet another level of control in regulating gene expression: interestingly, nickel binds to RNA but not to DNA or protein, suggesting that nickel also influences gene expression at the post-transcriptional level (Kaur and Dani 2003). It remains to be seen whether these levels of gene expression control are relevant in the upregulation of ABCB1 by nickel.

The upregulation of ABCB1 protected PTCs against nickel toxicity by extruding ceramides. Application of an ABCB1 inhibitor, PSC833, led to retention of ceramides in the cells and further attenuated cell viability (Fig. 4b, c). How ABCB1 transports the extremely hydrophobic ceramide remains to be investigated. The source of ceramides appears to be from the de novo ceramide synthesis pathway since cell viability improved with inhibitors of this pathway (Fig. 2c, Table 2). Moreover, the increase in the ceramide pool seems to drive the formation of GluCer, which also acts in a proapoptotic manner. One could hypothesize that an enlarged ceramide pool would also permit augmented levels of other ceramide metabolites, such as sphingosine, sphingosine-1-phosphate, sphingomyelin or ceramide-1-phosphate that contribute to cell fate decisions. While we cannot rule out roles for these metabolites in nickel toxicity or carcinogenesis, our data convincingly demonstrate that, in addition to ceramide, GluCer is a proapoptotic sphingolipid (Fig. 5). Furthermore, it has previously been

shown that ABCB1 can also transport glycosphingolipids, including GluCer (Lee et al. 2011; Eckford and Sharom 2005). Previously, Cabot and colleagues have reported that PSC833 induces ceramide formation (Cabot et al. 1998) and GCS regulates ABCB1 expression (Liu et al. 2001) in MCF7 breast cancer cells. In contrast, in normal renal PTCs, PSC833 alone has no effect on ceramide formation (Fig. 4c) and GCS siRNA did not affect ABCB1 expression (data not shown). These differing observations are probably due to the cell type used, that is, cancerous versus noncancerous.

In conclusion, we report several novel mechanisms in kidney cells: (1) nickel upregulates ABCB1 to improve cell survival; (2) nickel increases ROS and ceramide formation; (3) increased ceramides by nickel are extruded by ABCB1; and (4) GluCer is proapoptotic. The gained knowledge gives us an improved understanding of the molecular mechanisms involved in nickel toxicity and carcinogenesis of the kidney. Since environmental exposures normally consist of mixtures of heavy metals, it would be important to ascertain whether this mechanism is also applicable to other toxic and carcinogenic metals, such as chromium, lead and mercury.

Acknowledgments We thank Dr. Michael M. Gottesman (Laboratory of Cell Biology, National Cancer Institute, Bethesda, MD) and Dr. Ulrich Hopfer (Department of Physiology & Biophysics, Case Western Reserve University, Cleveland, OH) for providing ABCB1-MDCK and rat proximal tubule cell lines, respectively, Sanofi-Aventis for providing PSC833, and B. Scharner and S. Probst for expert technical assistance. F.D. received a fellowship from the Algerian Ministry for Higher Education. This work was funded by a University of Witten/Herdecke internal research program grant (to W.-K.L), the Westermann-Westdorp Foundation (to W.-K.L) and the Deutsche Forschungsgemeinschaft (TH345 10-1 and 11-1 to F.T.).

Conflicts of interest None.

References

Arena VC, Sussman NB, Redmond CK, Costantino JP, Trauth JM (1998) Using alternative comparison populations to assess occupation-related mortality risk. Results for the high nickel alloys workers cohort. J Occup Environ Med 40(10):907–916

Baker EK, Johnstone RW, Zalcberg JR, El-Osta A (2005) Epigenetic changes to the MDR1 locus in response to chemotherapeutic drugs. Oncogene 24(54):8061–8075. doi:10.1038/sj.onc.1208955

Baylin SB (2005) DNA methylation and gene silencing in cancer. Nat Clin Pract Oncol 2(Suppl 1):S4–11. doi:10.1038/ncponc0354

Bligh EG, Dyer WJ (1959) A rapid method of total lipid extraction and purification. Can J Biochem Physiol 37(8):911–917

Bork U, Lee WK, Kuchler A, Dittmar T, Thévenod F (2010) Cadmium-induced DNA damage triggers G(2)/M arrest via chk1/2 and cdc2 in p53-deficient kidney proximal tubule cells. Am J Physiol Renal Physiol 298(2):F255–F265. doi:10.1152/ajprenal.00273.2009

Bradford MM (1976) A rapid and sensitive method for the quantitation of microgram quantities of protein utilizing the principle of protein-dye binding. Anal Biochem 72:248–254

Brocato J, Costa M (2013) Basic mechanics of DNA methylation and the unique landscape of the DNA methylome in metal-induced carcinogenesis. Crit Rev Toxicol 43(6):493–514. doi:10.3109/10408444.2013.794769

Cabot MC, Han TY, Giuliano AE (1998) The multidrug resistance modulator SDZ PSC 833 is a potent activator of cellular ceramide formation. FEBS Lett 431(2):185–188

Chakraborty PK, Lee WK, Molitor M, Wolff NA, Thévenod F (2010) Cadmium induces Wnt signaling to upregulate proliferation and survival genes in sub-confluent kidney proximal tubule cells. Mol Cancer 9(1):102. doi:10.1186/1476-4598-9-102

Chen H, Ke Q, Kluz T, Yan Y, Costa M (2006) Nickel ions increase histone H3 lysine 9 dimethylation and induce transgene silencing. Mol Cell Biol 26(10):3728–3737. doi:10.1128/MCB.26.10.3728- 3737.2006

Chin KV, Tanaka S, Darlington G, Pastan I, Gottesman MM (1990) Heat shock and arsenite increase expression of the multidrug resistance (MDR1) gene in human renal carcinoma cells. J Biol Chem 265(1):221–226

Cortijo J, Milara J, Mata M, Donet E, Gavara N, Peel SE, Hall IP, Morcillo EJ (2010) Nickel induces intracellular calcium mobilization and pathophysiological responses in human cultured airway epithelial cells. Chem Biol Interact 183(1):25–33. doi:10.1016/j.cbi.2009.09.011

Costa M (2000) Chromium and nickel. In: Zalups RK, Koropatnick J (eds) Molecular biology and toxicology of metals. Taylor & Francis, London, pp 113–128

Cowart LA, Szulc Z, Bielawska A, Hannun YA (2002) Structural determinants of sphingolipid recognition by commercially available anti-ceramide antibodies. J Lipid Res 43(12):2042–2048

Cruz MT, Goncalo M, Figueiredo A, Carvalho AP, Duarte CB, Lopes MC (2004) Contact sensitizer nickel sulfate activates the transcription factors NF-kB and AP-1 and increases the expression of nitric oxide synthase in a skin dendritic cell line. Exp Dermatol 13(1):18–26. doi:10.1111/j.0906-6705.2004.00105.x

Ding J, He G, Gong W, Wen W, Sun W, Ning B, Huang S, Wu K, Huang C, Wu M, Xie W, Wang H (2009) Effects of nickel on cyclin expression, cell cycle progression and cell proliferation in human pulmonary cells. Cancer Epidemiol Biomarkers Prev 18(6):1720–1729. doi:10.1158/1055-9965.EPI-09-0115

Eckford PD, Sharom FJ (2005) The reconstituted P-glycoprotein multidrug transporter is a flippase for glucosylceramide and other simple glycosphingolipids. Biochem J 389(Pt 2):517–526. doi:10.1042/BJ20050047

Golebiowski F, Kasprzak KS (2005) Inhibition of core histones acetylation by carcinogenic nickel(II). Mol Cell Biochem 279(1–2):133–139. doi:10.1007/s11010-005-8285-1

Gottesman MM, Ling V (2006) The molecular basis of multidrug resistance in cancer: the early years of P-glycoprotein research. FEBS Lett 580(4):998–1009. doi:10.1016/j.febslet.2005.12.060

Gottesman MM, Fojo T, Bates SE (2002) Multidrug resistance in cancer: role of ATP-dependent transporters. Nat Rev Cancer 2(1):48–58. doi:10.1038/nrc706

Grassme H, Jekle A, Riehle A, Schwarz H, Berger J, Sandhoff K, Kolesnick R, Gulbins E (2001) CD95 signaling via ceramide-rich membrane rafts. J Biol Chem 276(23):20589–20596. doi:10.1074/jbc.M101207200

Gupta SC, Hevia D, Patchva S, Park B, Koh W, Aggarwal BB (2012) Upsides and downsides of reactive oxygen species for cancer: the roles of reactive oxygen species in tumorigenesis, prevention, and therapy. Antioxid Redox Signal 16(11):1295–1322. doi:10.1089/ars.2011.4414

Hanahan D, Weinberg RA (2011) Hallmarks of cancer: the next generation. Cell 144(5):646–674. doi:10.1016/j.cell.2011.02.013

Handlogten ME, Shiraishi N, Awata H, Huang C, Miller RT (2000) Extracellular Ca(2 +)-sensing receptor is a promiscuous divalent

cation sensor that responds to lead. Am J Physiol Renal Physiol 279(6):F1083–F1091
Hannun YA, Obeid LM (2008) Principles of bioactive lipid signalling: lessons from sphingolipids. Nat Rev Mol Cell Biol 9(2):139–150. doi:10.1038/nrm2329
Hartmann D, Lucks J, Fuchs S, Schiffmann S, Schreiber Y, Ferreiros N, Merkens J, Marschalek R, Geisslinger G, Grosch S (2012) Long chain ceramides and very long chain ceramides have opposite effects on human breast and colon cancer cell growth. Int J Biochem Cell Biol 44(4):620–628. doi:10.1016/j.biocel.2011.12.019
IARC (2012) Nickel and Nickel Compounds. A review of human carcinogens. Part C: Arsenic, metals, fibres, and dusts/IARC Working Group on the Evaluation of Carcinogenic Risks to Humans (2009: Lyon, France), vol 100C. International Agency for Research on Cancer, Lyon, France
Kasprzak KS, Jaruga P, Zastawny TH, North SL, Riggs CW, Olinski R, Dizdaroglu M (1997) Oxidative DNA base damage and its repair in kidneys and livers of nickel(II)-treated male F344 rats. Carcinogenesis 18(2):271–277
Kasprzak KS, Sunderman FW Jr, Salnikow K (2003) Nickel carcinogenesis. Mutat Res 533(1–2):67–97
Kaur P, Dani HM (2003) Carcinogenicity of nickel is the result of its binding to RNA and not to DNA. J Environ Pathol Toxicol Oncol 22(1):29–39
Lee SH, Choi JG, Cho MH (2001) Apoptosis, bcl2 expression, and cell cycle analyses in nickel(II)-treated normal rat kidney cells. J Korean Med Sci 16(2):165–168
Lee WK, Torchalski B, Thévenod F (2007) Cadmium-induced ceramide formation triggers calpain-dependent apoptosis in cultured kidney proximal tubule cells. Am J Physiol Cell Physiol 293(3):C839–C847
Lee WK, Torchalski B, Kohistani N, Thévenod F (2011) ABCB1 Protects Kidney Proximal Tubule Cells Against Cadmium-Induced Apoptosis: roles of Cadmium and Ceramide Transport. Toxicol Sci 121(2):343–356. doi:10.1093/toxsci/kfr071
Lee WK, Chakraborty PK, Roussa E, Wolff NA, Thévenod F (2012) ERK1/2-dependent bestrophin-3 expression prevents ER-stress-induced cell death in renal epithelial cells by reducing CHOP. Biochim Biophys Acta 1823(10):1864–1876. doi:10.1016/j.bbamcr.2012.06.003
Lee WK, Chakraborty PK, Thévenod F (2013) Pituitary homeobox 2 (PITX2) protects renal cancer cell lines against doxorubicin toxicity by transcriptional activation of the multidrug transporter ABCB1. Int J Cancer 133(3):556–567. doi:10.1002/ijc.28060
Littlefield NA, Fullerton FR, Poirier LA (1991) Hydroxylation and deglycosylation of 2′-deoxyguanosine in the presence of magnesium and nickel. Chem Biol Interact 79(2):217–228
Liu YY, Han TY, Giuliano AE, Cabot MC (2001) Ceramide glycosylation potentiates cellular multidrug resistance. FASEB J 15(3):719–730. doi:10.1096/fj.00-0223com
Mesicek J, Lee H, Feldman T, Jiang X, Skobeleva A, Berdyshev EV, Haimovitz-Friedman A, Fuks Z, Kolesnick R (2010) Ceramide synthases 2, 5, and 6 confer distinct roles in radiation-induced apoptosis in HeLa cells. Cell Signal 22(9):1300–1307. doi:10.1016/j.cellsig.2010.04.006
Park MA, Mitchell C, Zhang G, Yacoub A, Allegood J, Haussinger D, Reinehr R, Larner A, Spiegel S, Fisher PB, Voelkel-Johnson C, Ogretmen B, Grant S, Dent P (2010) Vorinostat and sorafenib increase CD95 activation in gastrointestinal tumor cells through a Ca(2 +)-de novo ceramide-PP2A-reactive oxygen species-dependent signaling pathway. Cancer Res 70(15):6313–6324. doi:10.1158/0008-5472.CAN-10-0999
Perry DK, Bielawska A, Hannun YA (2000) Quantitative determination of ceramide using diglyceride kinase. Methods Enzymol 312:22–31
Salnikow K, An WG, Melillo G, Blagosklonny MV, Costa M (1999a) Nickel-induced transformation shifts the balance between HIF-1 and p53 transcription factors. Carcinogenesis 20(9):1819–1823
Salnikow K, Kluz T, Costa M (1999b) Role of Ca(2 +) in the regulation of nickel-inducible Cap43 gene expression. Toxicol Appl Pharmacol 160(2):127–132. doi:10.1006/taap 1999.8759
Schinkel AH, Kemp S, Dolle M, Rudenko G, Wagenaar E (1993) N-glycosylation and deletion mutants of the human MDR1 P-glycoprotein. J Biol Chem 268(10):7474–7481
Scotto KW (2003) Transcriptional regulation of ABC drug transporters. Oncogene 22(47):7496–7511. doi:10.1038/sj.onc.1206950
Severa J, Vyskocil A, Fiala Z, Cizkova M (1995) Distribution of nickel in body fluids and organs of rats chronically exposed to nickel sulphate. Hum Exp Toxicol 14(12):955–958
Smith JC, Hackley B (1968) Distribution and excretion of nickel-63 administered intravenously to rats. J Nutr 95(4):541–546
Sunderman FW Jr, Maenza RM, Hopfer SM, Mitchell JM, Allpass PR, Damjanov I (1979) Induction of renal cancers in rats by intrarenal injection of nickel subsulfide. J Environ Pathol Toxicol 2(6):1511–1527
Tchou-Wong KM, Kiok K, Tang Z, Kluz T, Arita A, Smith PR, Brown S, Costa M (2011) Effects of nickel treatment on H3K4 trimethylation and gene expression. PLoS One 6(3):e17728. doi:10.1371/journal.pone.0017728
Thévenod F, Friedmann JM, Katsen AD, Hauser IA (2000) Up-regulation of multidrug resistance P-glycoprotein via nuclear factor-kappaB activation protects kidney proximal tubule cells from cadmium- and reactive oxygen species-induced apoptosis. J Biol Chem 275(3):1887–1896
Thévenod F, Wolff NA, Bork U, Lee WK, Abouhamed M (2007) Cadmium induces nuclear translocation of beta-catenin and increases expression of c-myc and Abcb1a in kidney proximal tubule cells. Biometals 20(5):807–820. doi:10.1007/s10534-006-9044-9
Toth M, Boros IM, Balint E (2012) Elevated level of lysine 9-acetylated histone H3 at the MDR1 promoter in multidrug-resistant cells. Cancer Sci 103(4):659–669. doi:10.1111/j.1349-7006.2012.02215.x
Vielhaber G, Brade L, Lindner B, Pfeiffer S, Wepf R, Hintze U, Wittern KP, Brade H (2001) Mouse anti-ceramide antiserum: a specific tool for the detection of endogenous ceramide. Glycobiology 11(6):451–457
Wang YF, Shyu HW, Chang YC, Tseng WC, Huang YL, Lin KH, Chou MC, Liu HL, Chen CY (2012) Nickel (II)-induced cytotoxicity and apoptosis in human proximal tubule cells through a ROS- and mitochondria-mediated pathway. Toxicol Appl Pharmacol 259(2):177–186. doi:10.1016/j.taap.2011.12.022
Wartenberg M, Ling FC, Muschen M, Klein F, Acker H, Gassmann M, Petrat K, Putz V, Hescheler J, Sauer H (2003) Regulation of the multidrug resistance transporter P-glycoprotein in multicellular tumor spheroids by hypoxia-inducible factor (HIF-1) and reactive oxygen species. FASEB J 17(3):503–505. doi:10.1096/fj.02-0358fje
Won JS, Singh I (2006) Sphingolipid signaling and redox regulation. Free Radic Biol Med 40(11):1875–1888. doi:10.1016/j.freeradbiomed.2006.01.035
Yang Y, Karakhanova S, Werner J, Bazhin AV (2013) Reactive oxygen species in cancer biology and anticancer therapy. Curr Med Chem 20(30):3677–3692